Atmospheric effects of biomass burning in Madagascar

Arthur C. Aikin, Walter R. Hoegy
Goddard Space Flight Center,
Greenbelt, Maryland

Jerry R. Ziemke
SGT, Greenbelt, Maryland

Arthur Thorpe
Howard University, Washington, D.C.

Abstract

Simultaneous tropospheric ozone and aerosols observed using the TOMS satellite instrument are reported for Madagascar during the 1979 through 1999 time period. Ozone observations made using the TOMS tropospheric ozone convective-cloud differential method show that the tropospheric ozone amount associated with Madagascar has an average monthly value of 30 DU (Dobson units). The average value is enhanced by 10 to 15 DU in October. This maximum coincides with the time of maximum biomass area burning in Madagascar and parts of southern Africa. The aerosol index derived from TOMS is examined for correlation with biomass burning in Madagascar and southern Africa. There is good correlation between a satellite observation derived fire index for different parts of Madagascar, tropospheric ozone and the TOMS aerosol index in the same geographical area. Aerosols from fires were found to reach their peak in November and to persist over Madagascar until sometime in December.

Introduction

There is extensive seasonal biomass burning in the equatorial regions of South America, Africa, and Asia [Justice et al., 1996; Fujiwara et al., 1999; Stroppiana et al., 2000; Dwyer et al., 2000]. These fires are connected to the growing season and as a result have a seasonal dependence, which is unique at each location [Cahoon et al., 1992]. Fires are known to produce large quantities of aerosols and trace gases such as carbon monoxide, nitrogen oxides and hydrocarbons [Scholes et al., 1996] The trace gas emissions lead to the production of ozone [Browell et al., 1996]. Trace gas and aerosol products from fires have been projected to have global impact [Crutzen and Andreae, 1990]. Madagascar is unique in that it is an island where more than 60%

of the area is systematically burned in September and October. The effect of this burning on the regional tropospheric ozone and aerosol burden is examined using a unique data set of the total tropospheric ozone and a measure of the aerosol content for the period 1979 to 2000. These data were observed with the TOMS satellite instrument. Other seasonal phenomena are also detailed.

Tropospheric ozone observations using TOMS

Tropospheric ozone can be derived from the TOMS total ozone measurement using the convective-cloud differential method [Ziemke et al., 19981. The principal of operation makes use of the difference between column ozone amount measured directly above a large convective cloud and the ozone amount in the vicinity of the cloud. In the first instance the reflection point is the cloud top. In the latter case the Earth's surface is the reflection surface. The ozone column difference corresponds to the amount of ozone between the cloud top and the surface.

The TOMS tropospheric ozone record extends from the beginning of 1979 to the present with a gap from May 1993 through June 1996. Figure 1 presents the monthly mean tropospheric column ozone for the location 12.5S and 47.5E, a location in the Mozambique Channel near Madagascar. This location is the center of a box 5 degrees on a side. The record shows a strong seasonal dependence with a maximum in October of each year. Maxima are greater in some years than others. The maximum tropospheric ozone ranges between 40 and 50 DU There are two exceptional years, 1987, when the maximum reaches 56 DU and 1997 when the largest amount was 51 DU. El Nino occurred in 1997 and modified the tropical tropospheric ozone. Tropospheric ozone increased over the western Pacific and decreased over the eastern Pacific [Chandra et al., 1998]. This is consistent with the observations over Madagascar. The minimum amount of tropospheric ozone lies between 20 and 30 DU. The minima occur in January and February following a steep decline from the October maximum. There is a secondary minimum in July to September. In some years the summer minimum is the lowest tropospheric ozone observed during the year.

The TOMS Aerosol Index

Absorbing tropospheric particles are detected by the TOMS instrument [Torres et al., 1998]. The operating principle of the TOMS instrument is based on measuring the attenuation of solar near ultraviolet radiation (330-340nm and 380-390nm) as it passes through the atmosphere and is reflected by the Earth's surface or clouds. The derived optical depth contains absorption by aerosols and ozone as well as Rayleigh scattering of photons. This leads to an aerosol index, which is a measure of the particle content [Herman et al., 1997; Torres et al., 1998]. In Figure 1 the aerosol index is plotted for the same location at 12.5'S and 47.5'E. There is a maximum in the index between September and November and another maximum in March from 1979 to 1994, the latter is quite variable from year to year in contrast to the Fall maximum. From 1996 to 2000 there is reduced evidence for the existence of a maximum at times other than the October-November period. Data from 1979 to 1993 were taken with a TOMS instrument on the Nimbus 7 spacecraft, while the 1997 to 2000 series was obtained with a different instrument on the EP-TOMS spacecraft. Because the wavelength separation used for aerosol analysis on Nimbus 7 TOMS was 4.0 nm versus 2.9 nm on EP-TOMS, the Nimbus 7 instrument was 1.25 more sensitive than the EP-TOMS instrument. This accounts for the differences in aerosol behavior seen in the different time periods. Towards the end of its lifetime the Nimbus 7 instrument experienced an instrument drift. This may account for the rise in aerosol index. Many of the maxima outside the Fall maximum are low values and have larger uncertainties associated with them. The appearance of aerosols in the Mozambique channel in the November time period has also been observed using the POLDER instrument on the ADEOS 1 spacecraft [Deuze et al., 1999].

Figure 2 shows for the same location and time period January 1992 to April 1993 a comparison of the aerosol index with tropospheric ozone for a shorter time period. The ozone exhibits a maximum in September through October. The peak ozone amount occurs at the time of the peak aerosol index values in September-November. From November through February the ozone amount declines and does not begin to recover until March. There is a secondary ozone maximum in March.

Biomass Burning in Madagascar and Southern Africa

Images from several satellites including DMSP and GOES are now routinely analyzed for biomass burning [Dwyer, 1998, 2000; Justice et al., 1996; Stoppiana et al., 2000; Elvidge et al., 2000]. Some of the data are available on the World Wide Web, for example the NOAA, NASA and ESA sites. Monthly statistics

are available for Africa for 1998-99. For Madagascar the maximum burning period is October. In the southern part of Africa the maximum burning occurs in October, the same time as in Madagascar [Hao and Liu, 1994]. Worldwide the maximum burning occurs in July.
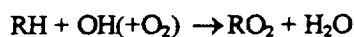
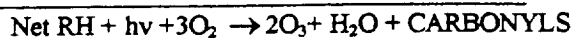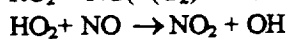**Comparison of Tropospheric Ozone, Aerosol Index and Fire Index for 1998 and 1999**

A map of the area from 8 S to 28 S and 38 E to 52 E, including the island of Madagascar is illustrated in Figure 3. The area is divided into 6 regions. All regions except region 1 include part of the island. The data plotted in Figures 1 and 2 represent area 2. Using data from the NOAA web site, a fire index normalized to the maximum fire count in region 2 has been derived for each of these quadrants for the period January 1998 through December 1999. This is plotted in Figure 4. This figure also contains the tropospheric ozone and aerosol index for each of these regions for the time period 1998-1999. The absence of a box representing a fire index means that the number of fires was too low to count or there were no fires. The number of fires and the aerosol index are multiplied by 40 to fit on the Dobson units plot. In regions 1 and 3 the maximum ozone occurs in September. Ozone peaks in September/October in region 4. November is the peak month for ozone in zones 5 and 6. Aerosols peak in November for every region except 1 where the peak is in October. There are clear fire maxima in November for region 2, and October for regions 4 and 5. Since fires reach their peak in September rather than October in southern Africa [Randriambelo et al., 1998], the ozone maximum in September in region 1 is probably the result of transport from Africa.

The aerosol index shows nearly the same temporal behavior in each of the different regions. The aerosol index is also correlated with the fire index, but with a time delay. Aerosols peak in November for all regions except region 1. The aerosol increase begins in August when the fire index first becomes meaningful. Aerosols are detected for several months after fires have been extinguished. The lag in aerosol detection may be related to the need for aerosols to be at a higher altitude before they can be detected by TOMS.

Discussion
The photochemical origin of tropospheric ozone utilizes $O(^1D)$ derived from ozone photodissociation to react with H_2O producing $2OH$. Thereafter the cycle is

$RH + OH(+O_2) \rightarrow RO_2 + H_2O$

$$RO_2 + NO(+(O_2)) \rightarrow NO_2 + HO_2 + CARBONYLS$$
$$HO_2 + NO \rightarrow NO_2 + OH$$
$$2[NO_2 + hv(O_2) \rightarrow NO + O_3]$$

$$Net\ RH + hv + 3O_2 \rightarrow 2O_3 + H_2O + CARBONYLS$$

See for example [Lelieveld and Dentener, 2000]. Here RH represents hydrocarbons and Carbonyls are hydrocarbon byproducts. The production of ozone depends on the presence of nitrogen oxides and hydrocarbons. Fires are a potent source of hydrocarbons. There are also large nitrogen oxide emissions during fires [Delmas et al., 1995]. Examination of satellite images shows that during the peak October/November burning season, there are numerous instances when convective cloud areas are present on Madagascar. Such systems provide vertical transport for gaseous and smoke fire product emissions. Convective cloud systems contribute NO_x through lightning activity [Price et al., 1997]. Although October is still in the Madagascar dry season, which lasts until late December, there is considerable lightning activity in both October and November as observed from orbit [Orville and Henderson, 1986]. Martin et al. [2000] estimate that 20% of the tropospheric ozone in this region comes from lightning. Biomass burning is accompanied by vertical transport. Observations at Reunion island show that the October ozone enhancement occurs above 4 km [Taupin et al., 1999]. Convective systems contribute to lifting fire products to this level.

Reunion Island (21°S, 55°E) is at the same latitude and 5° to 7° degrees east of Madagascar. Instrumented balloon launches from Reunion provide ozone profiles for the period 1992 through 1998 [Randriambo et al., 2000]. Although there is a gap in the TOMS ozone record from 1993 through 1995, there is overlap with the balloon observations in 1992, and 1996-1998. During these years at Reunion the mean ozone outside the Spring period is 30 DU. During Spring ozone is 45 DU. This is in general agreement with the TOMS observations except for 1997, when the TOMS Spring value is 56 DU.

Ozone is enhanced between 25 and 33% during the spring burning season. This increase is in agreement with recent estimates. Galanter et al., [2000] estimate that for the Madagascar region, tropospheric ozone would be 35 to 37.5 DU. This estimate is close to the amount observed during the 3 years when the October value was 40 DU, but is below the amount of other years in the data set shown in Figure 1 when the value was greater than 40 DU. An estimate of 20% for the contribution due to biomass burning has been made by Lelieveld and Dentener [2000].

The-aerosol index is a good indicator of smoke from biomass burning on the time scale of monthly averages. The spatial scale of 5 by 5 degrees is adequate for detection. Detailed validation is required to establish the size distribution and altitude of the smoke particles. There does not appear to be a clear photochemical association between the aerosols and tropospheric ozone as would be the case if the particles were acting as an ozone sink. The aerosol results support the view of Marufu et al. [2000] that the maximum effect of global biomass burning will occur over Madagascar in the December to May period. The March aerosol maximum may be explained in this way. However, the ozone results have their maximum in October at the time of local biomass burning.

Conclusions

The tropospheric ozone as measured by TOMS over Madagascar has a seasonal low between 20 to 30 DU during the period 1979 to 2000. The average yearly value outside the biomass burning period is 30 DU. Each October there is a maximum in the tropospheric ozone amounting to an enhancement of 10 to 15 DU. If all of this increase is attributed to fires, then biomass burning accounts for between 20 and 33% of the Fall tropospheric ozone levels above Madagascar. The presence of storms increased convection of fire products to altitudes above the boundary layer and above the region of lightning produced nitric oxide. The 1997 ozone October maximum was 51 DU, a value more than every other year except 1987, when the maximum was 56 DU. The aerosol index also increased in Fall 1997. Increased transport from the African continent or Indonesia may have contributed to aerosol and ozone loading. The occurrence of El Nino in 1997 may have changed transport. El Nino years are dryer, so there may have been more fires. The accompanying October maximum in the TOMS aerosol index, which is sensitive to smoke from biomass burning, supports increased burning.

References

Browell, E. V., et al., Ozone and aerosol distributions and air mass characteristics over the South Atlantic Basin during the burning season, *J. Geophys. Res.*, *101*, 24,043-24,068, 1996.

Cahoon, D. R., B. J. Stokes, J. S. Levine, W. R. Cofer, and K. P. O'Neil, Seasonal distribution of African savanna fires, *Nature, 359*, 812-815, 1992.

Chandra, S., J. R. Ziemke, W. Min, and W. G. Read, Effects of 1997-1998 El Nino on tropospheric ozone and water vapor, *Geophys. Res. Lett., 25*, 3867-3870, 1998.

Crutzen, P. J. and M. O. Andreae, Biomass burning in the tropics: Impact on atmospheric chemistry and biogeochemical cycles, *Science*, *250*, 1669-1618, 1990.

Delmas, R., J. P. Lacaux, J. C. Menaut, L. Abbadie, X. Le Roux, G. Helas, and J. Lobert, Nitrogen compound emission from biomass burning in tropical African savanna FOS/DECAFE 1991 Experiment (Lamto, Ivory Coast), *J. Atmos. Chem.*, *22*, 175-193, 1995.

Deuze, J. L., M. Herman, P. Goloub, D. Tanre, and A. Marchand, Characterization of aerosols over ocean from POLDER/ADEOS-1, *Geophys. Res. Lett.*, *26*, 142 1 1424, 1999.

Dwyer, E., J-M. Gregoire, and J. P. Malingreau, A global analysis of vegetation fires using satellite images: spatial and temporal dynamics, *AMBIO*, *27*, 175-181, 1998.

Dwyer, E., S. Pinnock, and J-M. Gregoire, Global, spatial, and temporal distribution of vegetation fire as determined from satellite observations, *Int. J. Remote Sensing*, *21*, 1289-1302, 2000.

Elvidge, C. D., K. E. Baugh, V. R. Hobson, E. A. Kihn, and H. W. Kroehl, Detection of fires and power outages at night using DMSP-OLS data, NOAA web site, 2000.

Fujiwara, M., K. Kita, S. Kawakami, T. Ogawa, N. Komala, S. Saraspriya, and A. Suripto, Tropospheric ozone enhancements during the Indonesian forest fire events in 1994 and in 1997 as revealed by ground-based observations, *Geophys. Res. Lett.*, *26*, 2417-2420, 1999.

Galanter, M., H. Levy II, and G. R. Carmichael, Impacts of biomass burning on tropospheric CO, NO_x, and O_3, *J. Geophys. Res.*, *105*, 6633-6653, 2000.

Hao, W. M., and M.-H., Liu, Spatial and temporal distribution of tropical biomass burning, *Global Biogeochent Cycles*, *8*, 495-503, 1994.

Herman, J. R., P. K. Bhartia, O. Torres, N. C. Hsu, C. J. Seftor, and E. Celarier, Frequency of occurrence of absorbing aerosols, *J. Geophys. Res.*, *102*, 16,911-16,921, 1997.

Justice, C. O., J. D. Kendall, P. R. Dowty, and R. J. Scholes, Satellite remote sensing of fires during the SAFARI campaign using NOAA advanced very high resolution radiometer data, *J. Geophys. Res.*, *101*, 23,851-23,863, 1996.

Lelieveld, J., and F. J. Dentener, What controls tropospheric ozone?, *J. Geophys. Res.*, *105*, 3531-3551, 2000.

Martin, R. V., D. J. Jacob, J. A. Logan, J. M. Ziemke, and R. Washington, Detection of a lightning influence on tropical tropospheric ozone, *Geophys. Res. Lett.*, *27*, 1639-1642, 2000.

Marufu, L., F. Dentener, J. Lelieveld, M. O. Andreae, and G. Helas, Photochemistry of the African troposphere: Influence of biomass-burning emissions, *J. Geophys. Res.*, *105*, 14,513-14,530, 2000.

Orville, R. E. and R. W. Henderson, Global distribution of midnight lightning: September 1977 to August 1978, *Mon. Wea. Rev.*, *114*, 2640-2653, 1986.

Price, C., J. Penner, and M. Prather, NO, from lightning 1. Global distribution based on lightning physics, *J. Geophys. Res.*, *102*, 5929-5941, 1997.

Randriambo, T., S. Baldy,, M. Bessafi, M. Petit, and M. Despinoy, An improved detection and characterization of active fires and smoke

in southeastern Africa and Madagascar, *Int J. Remote Sens.*, *19*, 2623-2638, 1998.

Randriambo, T., J.-L. Baray, and S. Baldy, effect of biomass burning convective venting,and transport of tropospheric ozone over the Indian Ocean: Reunion Island field observations *J. Geophys. Res.*, *105*, 11,813-11,832, 2000.

Schole, R. D., D. E. Ward, and C. O. Justice, Emissions of trace gases and aerosol particles due to vegetation burning in southern hemisphere Africa, *J. Geophys. Res.*, *101*, 23,677-23,682, 1996.

Stroppiana, D., S. Pinnock, and J.-M. Greaoire, The Global Fire Product: daily fire occurrence from April 1992 to December 1993 derived from NOAA AVHRR data, *Int. J. Remote Sens.*, *21*, 1279-12889, 2000.

Taupin, F. G., M. Bessafi, S. Baldy, and P. J. Bremaud, Tropospheric ozone above the southwestern Indian Ocean is strongly linked to dynamical conditions prevailing in the tropics, *J. Geophys. Res.*, *104*, 8057-8066, 1999.

Torres, O., P. K. Bhartia, J. R. Herman, and Z. Ahmad, Derivation of aerosol properties from satellite measurements of backscattered ultraviolet radiation, : Theoretical basis, *J. Geophys. Res.*, *103*, 17,099-17,110, 1998.

Ziemke, J.R., S. Chandra, and P. K. Bhartia, Two new methods for deriving tropospheric column ozone from TOMS measurements: Assimilated UARS/MLS/HALOE and convective-cloud differential techniques, *J. Geophys. Res.*, *103*, 22,115-22,123, 1998.
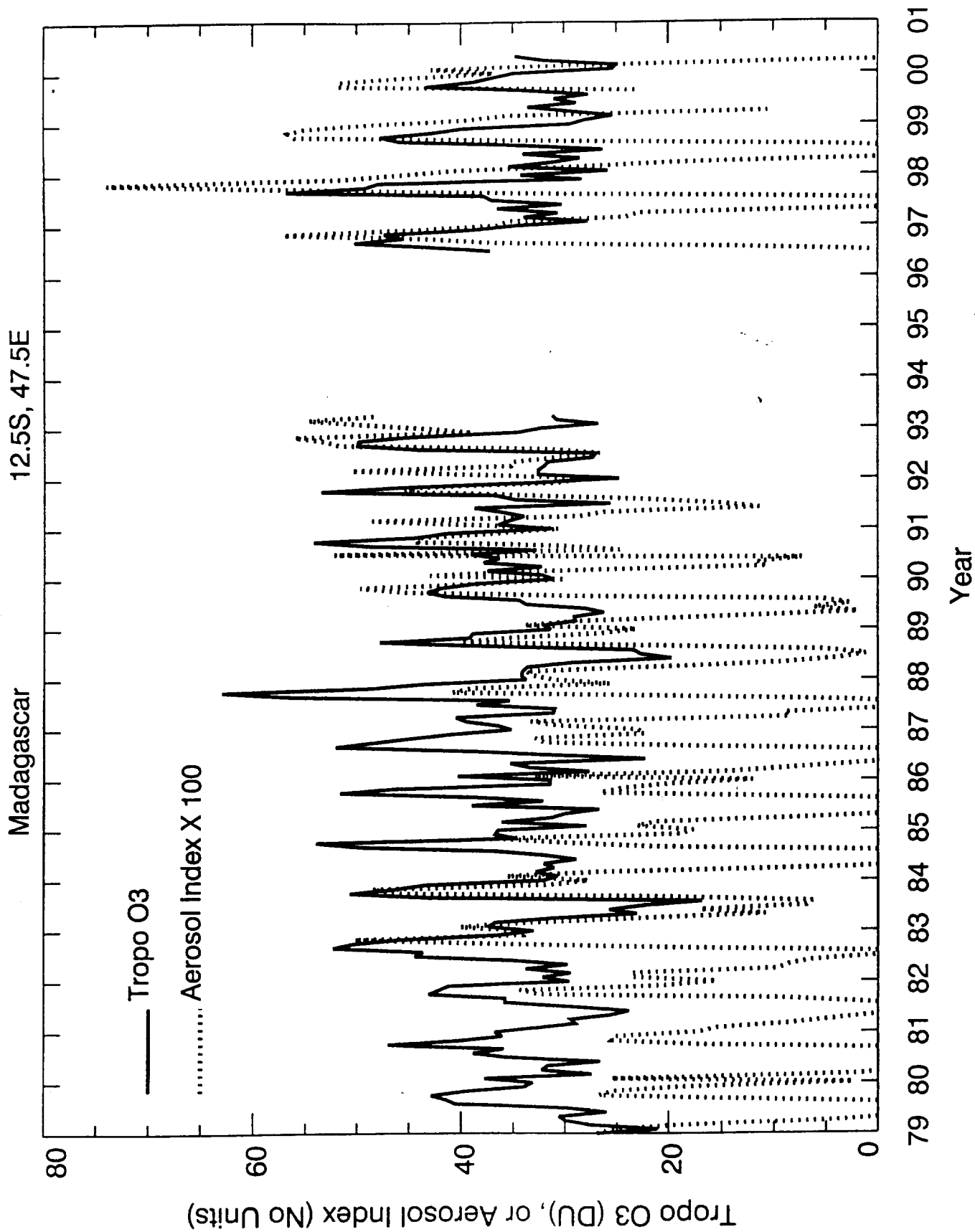
Figure 1. Tropospheric column ozone in DU for the period 1979 - 1999 at 12.5°S and 47.5°E in the Mozambique Channel between Madagascar and Africa. Dark line indicates ozone. Dashed line represents aerosols.
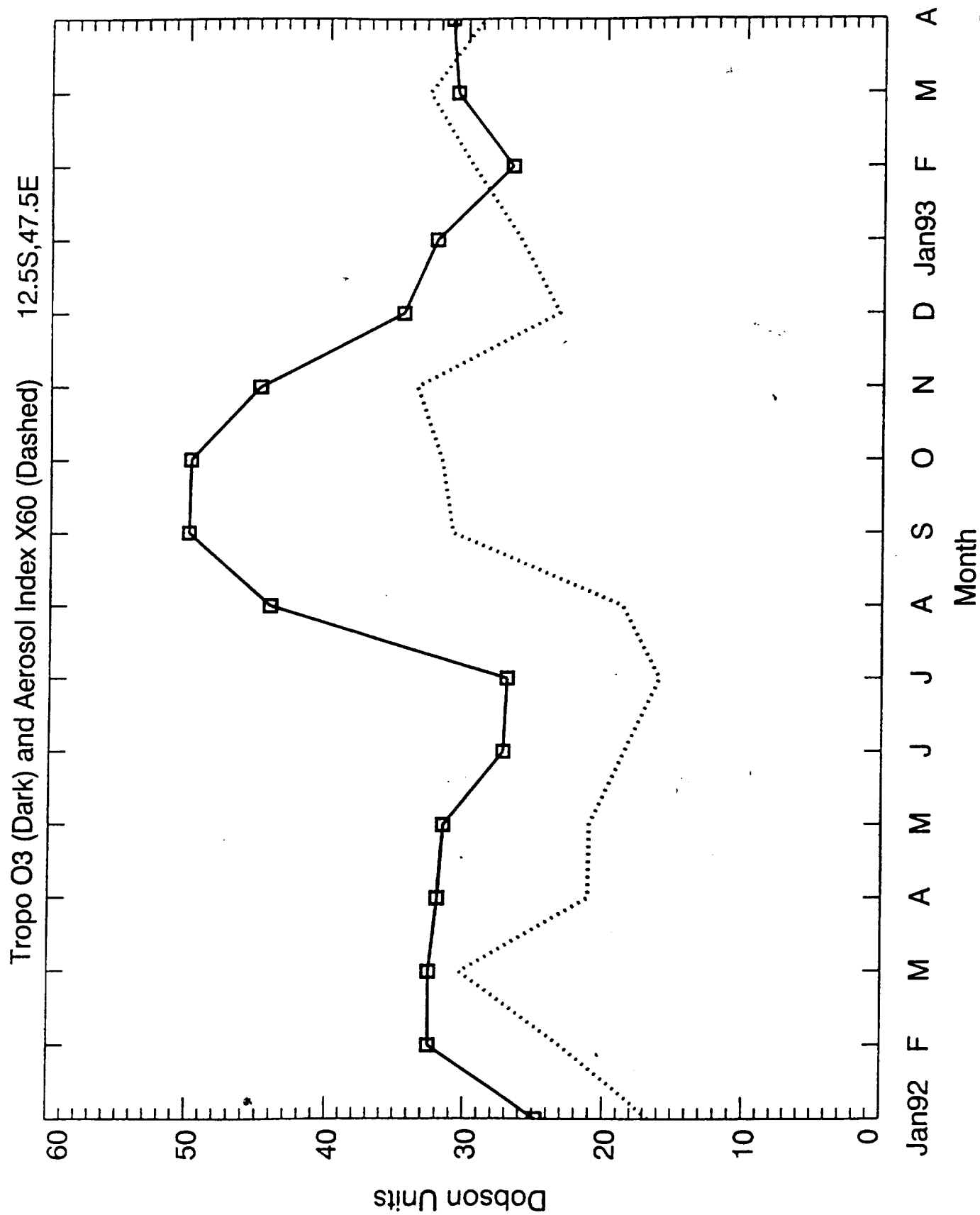
Figure 2. Tropospheric column ozone in DU for the period July 1992 to May 1993 at 12.5°S and 47.5°E (solid curve). Aerosol index for the same period (dotted curve).
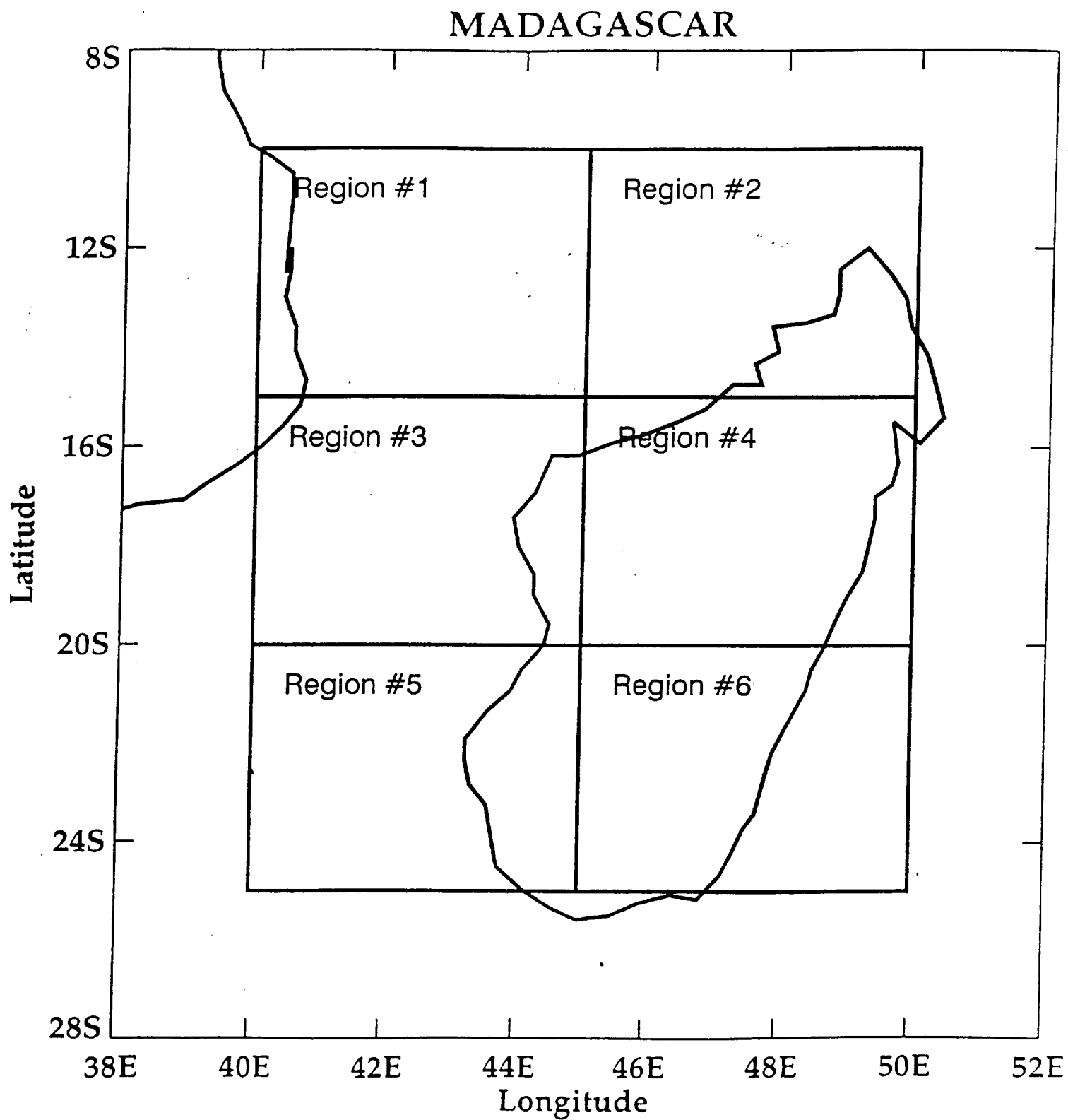
MADAGASCAR

Figure 3 Map of Madagascar showing geographic regions used in data comparisons.
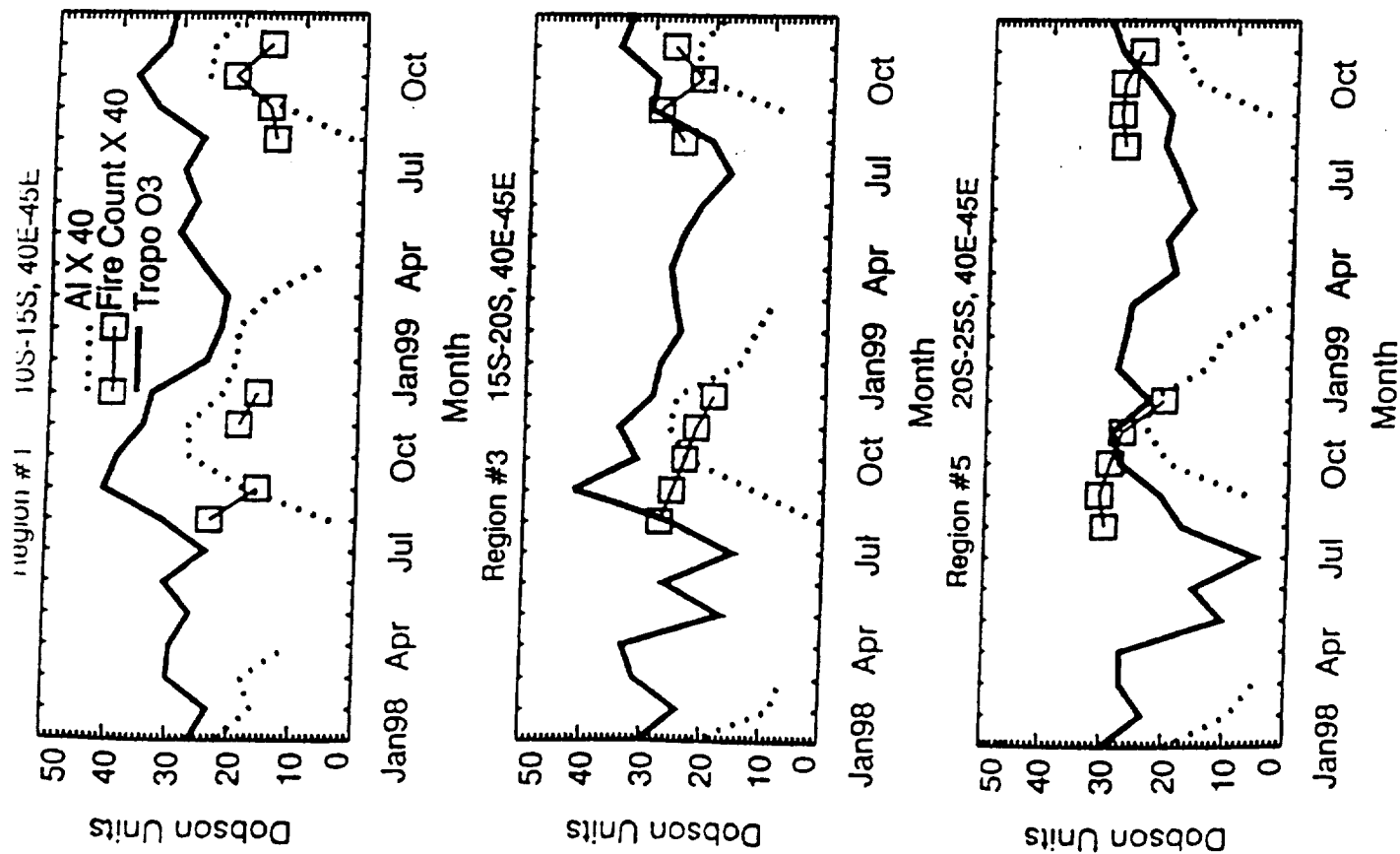
Figure 4 Comparison of TOMS tropospheric ozone (solid curve) aerosol index (dotted curve) and fire index (squares) for 1998 and 1999.